Studying the Internal Heat Transfer By Natural Convection Through an Inclined and a Modified Square Enclosure with a Triangular Top Wall.

Dr. Salam Hadi Hussain*
Mechanical Engineering Department- College of Engineering
Babylon University- Babylon City – Hilla – Iraq.
*** E-mail : salamphd1974@yahoo.com or salam.hh@i-acci.org**

ABSTRACT

A numerical analysis used to simulate laminar natural convective heat transfer in a two-dimensional inclined and a modified square enclosure having a triangular top wall has been performed. The model is applied to analyze natural convection in this enclosure where the left side wall is subjected to a constant heat flux while the other opposite wall is kept at isothermal cold temperature. The other enclosure walls are considered adiabatic. The enclosure under study is filled with air with Prandtl number is taken as **0.71**. The two-dimensional flow is solved numerically by using the Finite Volume Method (**FVM**).The computations are carried out at different heights of triangular top wall. The Rayleigh numbers considered ranging from $\mathbf{10^3}$ to $\mathbf{10^6}$. The effect of inclination angle of the enclosure on the resulting convection process is investigated for inclination angles ranging from $\mathbf{0^o}$ to $\mathbf{60^o}$. The results of the present investigation show that the convective phenomenon is greatly influenced by the inclined top wall height and the dominance of the convective currents with the increase of Rayleigh number and inclination angle. The streamline and isotherm plots and the variation of the average Nusselt number at the hot left side wall are also presented. The results showed a good agreement with another published results.

Keywords: Natural Convection, CFD , Constant Heat Flux , Enclosure, Laminar Flow, Triangular Top Wall.

الخلاصة :

التحليل العددي تم استخدامه لنمذجة انتقال الحرارة الطباقي بالحمل الحر خلال دهليز ثنائي البعد مائل مربع ومحور الشكل و يحتوي على سطح علوي ذا شكل مثلثيالبحث يتناول جريان المائع و سريان الحرارة في ذلك الدهليز حيث الجدار الجانبي الأيسر يكون معرضا لفيض حراري ثابت بينما الجدار الجانبي المقابل يكون بارداً.أما بقية جدران الدهليز فتكون معزولة حراريا.الدهليز قيد الدراسة مملوء بالهواء وبرقم براندل يساوي**0.71** .الجريان ثنائي البعد تم حله عدديا باستخدام طريقة الحجوم المحددة . الحسابات تم أجرائها لارتفاعات مختلفة للسطح العلوي المثلثي. رقم رايلي تم استخدامه لمدى يتراوح من $\mathbf{10^3}$ الى $\mathbf{10^6}$.تأثير زاوية ميلان الدهليز على عملية الحمل الحراري تم دراستها لمدى من زوايا الميلان يتراوح من **0** الى **60** درجة. نتائج الدراسة الحالية أوضحت بان ظاهرة الحمل الحراري تتأثر بشكل كبير بارتفاع السطح العلوي المائل وكذلك هيمنة تيارات الحمل بزيادة رقم رايلي وزاوية الميلان .تم عرض النتائج على هيئة أشكال لخطوط انسياب الجريان ودرجة الحرارة ورقم نسلت المتوسط عند الجدار الجانبي الأيسر الساخن .النتائج أوضحت تطابق جيد مع النتائج الأخرى المنشورة.

NOMENCLATURE:

Symbol	Description
a_1, a_2	*Transformation coefficients*
E	*Height of the inclined top wall , (m)*
F	*Control function*
g	*Gravitational acceleration,(m/s^2)*
J	*Jacobian of residual equations*
k	*Thermal conductivity of fluid, (W / m.°C)*
H	*Height of the enclosure, (m)*
L	*Width of the enclosure, (m)*
Nu_{av}	*Average Nusselt number*
n	*Outward flux normal to boundary*
P	*Dimensionless pressure*
p	*Pressure, (N/m^2)*
Pr	*Prandtl number*
Q	*Control function*
q	*Heat flux per unit area, (W/m^2)*
Ra	*Rayleigh number*
S_{ϕ}	*Linearized source term for* ϕ
T	*Temperature, (°C)*
T_c	*Temperature of the cold surface, (°C)*
U	*Dimensionless velocity component in x-direction*
u	*Velocity component in x-direction, (m/s)*
V	*Dimensionless velocity component in y-direction*
v	*Velocity component in y-direction, (m/s)*
X	*Dimensionless Coordinate in horizontal direction*
x	*Cartesian coordinate in horizontal direction, (m)*
Y	*Dimensionless Coordinate in vertical direction*
y	*Cartesian coordinate in vertical direction, (m)*
α	*Thermal diffusivity, (m^2/s)*
β	*Volumetric coefficient of thermal expansion, (K^{-1})*
θ	*Dimensionless temperature*
ϕ	*Variable vector*
γ	*Enclosure inclination angle with horizontal Direction, (degree)*
ν	*Kinematic viscosity of the fluid, (m^2/s)*
ρ	*Density of the fluid, (kg/m^3)*
ξ, η	*Dimensionless body-fitted coordinates*

1. INTRODUCTION

Natural convection is observed as a result of the motion of the fluid due to density changes arising from heating process. The movement of the fluid in natural convection results from the buoyancy forces imposed on the fluid when its density of the heat transfer surface is described as a result of thermal expansion of the fluid in a non-uniform temperature distribution. Convection heat transfer is dependent on the movement of the fluid and the development of the flow of the fluid is also affected by the shape of the heat transfer surfaces. Both numerical and experimental methods have been used to obtain the solution of heat transfer and fluid flow problems. In most cases, the experimental methods are costly and time consuming due to necessary of expensive prototypes and instrumentations. On the other hand, numerical methods can offer considerable savings in design time and cost **Saha [1]**, **2007**.The problem of convective heat transfer in an enclosure has been studied extensively because of the wide application of such process. The flow inside an enclosure is much more complicated to investigate, as the boundary zone and the middle core zone never have the same effect for a certain boundary condition considered. **Ali** and **Husain [2]**,**1993,** investigated the effect of corrugation frequencies on natural convective heat transfer and flow characteristics in a square enclosure of vee-corrugated vertical walls. This investigation showed that the overall heat transfer through the enclosure increased with the increase of corrugation for low Grashof number; but the effect was reversed for high Grashof number. **Ganzarolli** and **Milanez [3]** ,**1995,** performed a numerical study of steady natural convection in rectangular enclosures heated from below and symmetrically cooled from the sides. The size of the cavity was varied from square to shallow where the cavity width was varied from **1–10** times of the height. The heat source, which spanned the entire bottom wall, was either isothermal or at constant heat flux condition. They observed that, for the square cavity, the flow and thermal fields are not strongly affected by the isothermal or constant heat flux boundary condition at the bottom heat source. **Aydin** and **Yang [4]** , **2000 ,** investigated numerically the natural convection of air in a vertical square cavity with localized isothermal heating from below and symmetrical cooling from the sidewalls. The top wall as well as the non-heated parts of the bottom wall was considered adiabatic. The length of the symmetrically placed isothermal heat source at the bottom was varied. Their results showed that there a two counter rotating vortices were formed in the flow domain due to natural convection. **Sharif** and **Mohammad [5]** , **2005 ,** studied numerically natural convection in rectangular cavities by using a finite volume method. Their study was based on a configuration where a constant flux heat source was symmetrically embedded at the bottom wall.

The length of the heat source was varied from **20** to **80%** of the total length of the bottom wall. The non-heated parts of the bottom wall were considered adiabatic. The Grashof number was varied from $\mathbf{10^3}$ to $\mathbf{10^6}$. The effects of aspect ratio, inclination angles, and heat source length on the convection and heat transfer process in the cavity were analyzed. Results are presented in the form of streamline and isotherm plots as well as the variation of the Nusselt number and maximum temperature at the heat source surface under different conditions. **Sivasankaran [6]** , **2006,** presented a numerical study to analyze the effects of discrete heat sources on the natural convection of heat generating fluids contained in a square cavity with isothermal walls and the top and bottom perfectly insulated surfaces. The flow was assumed to be two-dimensional and calculations were carried out by solving governing equations using control volume method for different parameters. Results were presented graphically in the form of streamlines, isotherms and velocity profiles. It was observed that heater positioned at the bottom gave better heat transfer rate than others. **Kandaswamy** and **Sivasankaran [7]** , **2006,** studied natural convection in an inclined enclosure with internal heat generation . They found that the rate of heat transfer was increased when the source strength was increased. **Sathiyamoorthy et al. [8]** , **2007 ,** studied natural convection flow in a closed square cavity when the bottom wall was uniformly heated and vertical wall(s) were linearly heated while the top wall was well insulated. Non-linear coupled governing equations were solved by using penalty finite element method with bi-quadratic rectangular elements. Numerical results were obtained for various values of Rayleigh number and Prandtl number .Results were presented in the form of streamlines, isotherm contours, local Nusselt number and the average Nusselt as a function of Rayleigh number. **Kandaswamy et al. [9]** , **2007,** investigated numerically natural convection heat transfer in a square cavity induced by heated plate. Top and bottom of the cavity were considered adiabatic, while the two vertical walls of the cavity have a constant temperature lower than the plate's temperature. The flow was assumed to be two-dimensional and the discretized equations were solved by using finite difference method. Their study was performed for different values of Grashof number ranging from $\mathbf{10^3}$ to $\mathbf{10^5}$ and for different aspect ratios and position of heated plate. They found that when Grashof number increased ,the heat transfer rate increased in both vertical and horizontal position of the plate while, when aspect ratio of heated thin plate was decreased the heat transfer also decreased. **Natarajan et al. [10]** , **2008,** used a penalty finite element analysis to investigate the influence of uniform and non-uniform heating of bottom wall on natural convection flows in a trapezoidal cavity. The bottom wall was uniformly and non-uniformly heated while two vertical walls were maintained at constant cold temperature and the top wall was well insulated. They observed a symmetry while representing the flow patterns in terms of stream functions. Non-uniform heating of the bottom wall produced greater heat transfer rate at the center of the bottom wall than uniform heating case for all Rayleigh numbers but average Nusselt number showed overall lower heat transfer rate for non-uniform heating case. **Sultana et al. [11]**, **2008** presented a numerical study of natural convection by using a penalty finite element method in a tilted square cavity with heated horizontal base and cold upper wall. Their study was based on a configuration where the top triangular wall of two different shapes was maintained at a constant low temperature. A constant heat flux source whose length is **20%** of the total length of the cavity was discretely embedded at the left corner of the bottom wall while the remaining part of the bottom wall and the two sidewalls were considered to be adiabatic. Their study included computations for inclination angle of $\mathbf{45^o}$, while the Grashof number varies from $\mathbf{10^3}$ to $\mathbf{10^6}$. Their results explained that a significant effect of different triangular top surface on the heat transfer characteristics at the higher Grashof number and inclination angle. **Saha et al. [12], 2008,** carried out a numerical study for laminar natural convection heat transfer within a two-dimensional modified square enclosure having a triangular roof. The vertical sidewalls are differentially heated considering a constant flux heat source strip which was mounted with the left wall. The opposite wall is considered isothermal having a temperature of the surrounding fluid. The rest of the walls are adiabatic. Air is considered as the fluid inside the enclosure. The solution has been carried out on the basis of finite element analysis with different heights of the triangular roof. Fluid flow fields and isotherm patterns and the average Nusselt number were presented for the Rayleigh numbers ranging from $\mathbf{10^3}$ to $\mathbf{10^6}$ .They concluded that the convective phenomenon is greatly influenced by the inclined roof height. From the above literature survey, it was found that there are some limited studies for non-linear top or bottom walled enclosure. The main purpose of present study is to investigate the effect of the inclination angle on the heat transfer and fluid flow for natural convection inside a modified square inclined enclosure with a triangular top wall by considering the constant heat flux at one side of the vertical walls for different Rayleigh number ranging from $\mathbf{10^3}$ to $\mathbf{10^6}$. The other vertical wall is kept at a constant temperature and the rest of the walls, i.e. ,the bottom wall and triangular inclined top walls are at adiabatic condition. The present study is based on the configuration of **Saha et al. [12], 2008**.The main difference between **Saha et al. [12]** and the present work is that the present work deals with the inclined modified square enclosure using finite volume method rather than the vertical modified square enclosure using finite element method as in **Saha et al. [12]** work.

2. PROBLEM DESCRIPTION AND THE MATHEMATICAL ANALYSIS

The present model consists of a two-dimensional inclined modified square enclosure having a triangular top wall. The vertical side left wall is subjected to a constant heat flux while the opposite right wall is considered isothermal which having a temperature of the surrounding fluid. The rest of the walls are considered adiabatic. Air is considered as the fluid inside the enclosure with **Pr = 0.71**. The enclosure has the same height and width (**H = L**) and the top inclined triangular wall has the height **E** which is considered to have a length of **0.1** to **0.5** times **L** in the present study. The geometry under investigation is shown schematically in **Fig. (1).** Different heights of the triangular top wall have been considered for the present analysis. Fluid flow fields and isotherm patterns and the average Nusselt number are presented for the Rayleigh numbers ranging from $\mathbf{10^3}$ to $\mathbf{10^6}$ and the enclosure inclination angle, γ, is varied as $\mathbf{0^o}$, $\mathbf{20^o}$, $\mathbf{40^o}$ and $\mathbf{60^o}$ respectively. The numerical solution is obtained by using a finite volume scheme and the following assumptions are considered in the present analysis:-

1. The flow is considered laminar , steady and two-dimensional.

2.The fluid properties are assumed constant except for the density variation in the buoyancy term which is treated according to Boussinesq approximation.

3.The fluid inside the enclosure is assumed Newtonian and incompressible while viscous dissipation effects are considered negligible.

4. The model is assumed to be not subjected to any external flow; hence the internal natural convection phenomenon is studied for the present model.

5. All the solid boundaries are assumed to be rigid with no-slip condition.

The laminar internal two-dimensional flow and the temperature distribution inside the enclosure are described by the Navier–Stokes and the energy equations, respectively. The governing equations are transformed into a dimensionless forms by using the following dimensionless variables **[12]**:-

$$\theta = \frac{T - T_o}{q\ L/k}\ , \qquad X = \frac{x}{L} \quad , Y = \frac{y}{L} \qquad (1)$$

$$U = \frac{\mathrm{u\ L}}{\alpha} \quad , V = \frac{\mathrm{v\ L}}{\alpha} \quad , P = \frac{p\ L^2}{\rho\ \alpha^2} \qquad (2)$$

The dimensionless forms of the governing equations of steady two-dimensional internal laminar natural convection are expressed in the following forms **[12]**:-

$$\frac{\partial U}{\partial X} + \frac{\partial V}{\partial Y} = 0 \qquad (3)$$

$$U\frac{\partial U}{\partial X} + V\frac{\partial U}{\partial Y} = -\frac{\partial P}{\partial X} + Pr\left(\frac{\partial^2 U}{\partial X^2} + \frac{\partial^2 U}{\partial Y^2}\right) + Ra\,Pr\,\theta\ \sin(\gamma) \qquad (4)$$

$$U\frac{\partial V}{\partial X} + V\frac{\partial V}{\partial Y} = -\frac{\partial P}{\partial Y} + Pr\left(\frac{\partial^2 V}{\partial X^2} + \frac{\partial^2 V}{\partial Y^2}\right) + Ra\,Pr\,\theta\ \cos(\gamma) \qquad (5)$$

$$U\frac{\partial \theta}{\partial X} + V\frac{\partial \theta}{\partial Y} = \left(\frac{\partial^2 \theta}{\partial X^2} + \frac{\partial^2 \theta}{\partial Y^2}\right) \qquad (6)$$

Where **Pr** is the Prandtl number and ***Ra*** is the Rayleigh number. The previous dimensionless numbers are defined by **[12]**:-

$$Pr = \frac{\upsilon}{\alpha} \qquad and \qquad Ra = \frac{g\beta q L^4}{k\upsilon\alpha} \qquad (7)$$

The average Nusselt number, $\boldsymbol{Nu_{av}}$,at the hot left side wall is given by **[12]** :-

$$Nu_{av} = \frac{H}{L} \int_0^{L/H} \frac{1}{\theta(Y)}\, dY \qquad (8)$$

where $\theta(Y)$ is the dimensionless temperature at the hot left side wall.

3. BOUNDARY CONDITIONS

The boundary conditions which are used in the present study can be arranged as follows:-

1. The left side wall (i.e. surface **I**) is subjected to a constant heat flux **q** , so:-

X=0, $\frac{\partial\theta}{\partial X} = -1$ and U=V=0 **(9)**

2. The right side wall (i.e. surface **III**) is kept at a uniform cold temperature (**T_c**) so:-

X = 1, $\theta = 0$ and U = V = 0 **(10)**

3. The other surfaces of enclosure (i.e. surfaces **II , IV** and **V**) are thermally insulated so:

$\frac{\partial\theta}{\partial Y} = 0$ and $\frac{\partial\theta}{\partial n} = 0$, U = V = 0 **(11)**

4. NUMERICAL TECHNIQUE

In this section numerical method adopted in the present study is discussed.

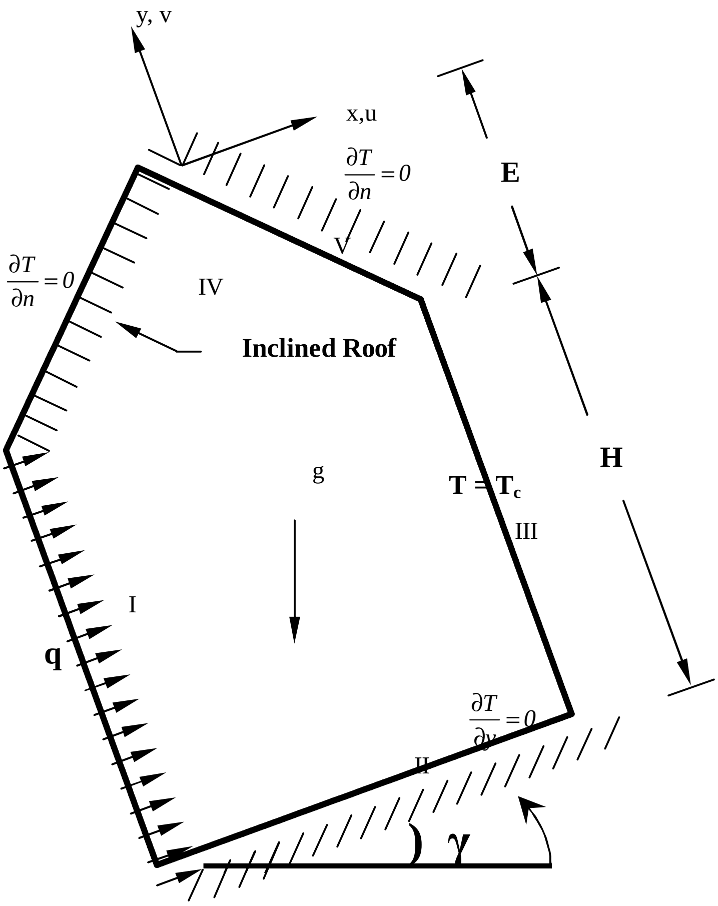

Figure 1: Schematic Physical Configuration and Boundary Conditions of the Modified and Inclined Square Enclosure

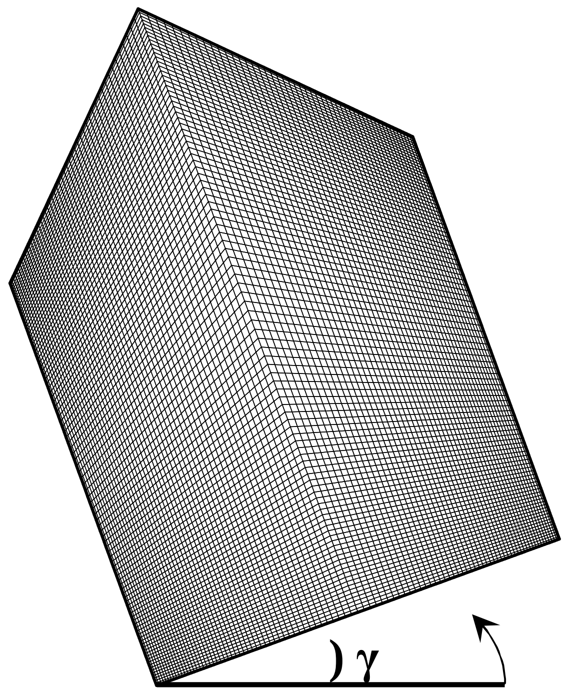

Figure 2: A Typical 2D - Grid Distribution (100 x 100) with Non-uniform and Non-orthogonal Distributions for Inclination Cavity .

4.1. GRID GENERATION

The grid generation calculation is based on the curvilinear coordinate system applied to fluid flow as described by **Thompson et al. [13]**. **Fig.(2)** shows the schematic of two dimensions body fitting grid used for the present computation. This grid is obtained by solving non-homogeneous 2-D Poisson equations [14]:-

$$\nabla^2 \xi = F(\xi,\eta) \qquad (12-a)$$

$$\nabla^2 \eta = Q(\xi,\eta) \qquad (12-b)$$

Define F and Q in the following formulae,

$$F = \frac{1}{h_1 h_2} f_\xi \quad and \quad Q = \frac{1}{h_1 h_2}\left(\frac{1}{f}\right)_\eta \qquad (12-c)$$

Where $h_1 = g_{11}^{1/2}$ and $h_2 = g_{22}^{1/2}$ $(12-d)$

$$f = \frac{h_2}{h_1} = \left(\frac{x_\eta^2 + y_\eta^2}{x_\xi^2 + y_\xi^2}\right)^{1/2} \qquad (12-e)$$

$$f_\xi = \frac{\left(\frac{x_\xi^2 + y_\xi^2}{x_\eta^2 + y_\eta^2}\right)^{1/2}(x_\eta x_{\eta\xi} + y_\eta y_{\eta\xi})}{x_\xi^2 + y_\xi^2} - \frac{\left(\frac{x_\eta^2 + y_\eta^2}{x_\xi^2 + y_\xi^2}\right)^{1/2}(x_\xi x_{\xi\xi} + y_\xi y_{\xi\xi})}{x_\xi^2 + y_\xi^2} \qquad (12-f)$$

$$\left(\frac{1}{f}\right)_\eta = \frac{\left(\frac{x_\eta^2 + y_\eta^2}{x_\xi^2 + y_\xi^2}\right)^{1/2}(x_\xi x_{\eta\xi} + y_\xi y_{\eta\xi})}{x_\eta^2 + y_\eta^2} - \frac{\left(\frac{x_\xi^2 + y_\xi^2}{x_\eta^2 + y_\eta^2}\right)^{1/2}(x_\eta x_{\eta\eta} + y_\eta y_{\eta\eta})}{x_\eta^2 + y_\eta^2} \qquad (12-g)$$

where F and Q are control functions used to cluster the grid near the walls .The reason is to sense the velocity gradient because there is a friction between the wall and the fluid. The equations are transformed to (ξ, η) coordinates by interchanging the roles of dependent variables. This yield the following system equations [14]:-

$$g_{11}x_{\xi\xi} - g_{21}x_{\xi\eta} + g_{22}x_{\eta\eta} = -J^2(Fx_\xi + Qx_\eta) \qquad (13-a)$$

$$g_{11}y_{\xi\xi} - g_{21}y_{\xi\eta} + g_{22}y_{\eta\eta} = -J^2(Fy_\xi + Qy_\eta) \qquad (13-b)$$

Where:

$$g_{11} = x_\eta^2 + y_\eta^2 \qquad (13-c)$$

$$g_{21} = 2(x_\xi x_\eta + y_\xi y_\eta) \qquad (13-d)$$

$$g_{22} = x_\xi^2 + y_\xi^2 \qquad (13-e)$$

$$J = x_\xi y_\eta - x_\eta y_\xi \qquad (13-f)$$

Eqs. (13-*a*) and (13-*b*) are solved by **SOR** method. All the derivatives are discretized using second order central difference scheme and the non-linearity is resolved through iterations. A typical generated grid is shown in **Fig. 2**.

4.2. DISCRETIZATION TECHNIQUE AND METHOD OF SOLUTION

The coupled governing equations (**3** to **6**) are transformed into sets of algebraic equations using finite volume method. The above equations are integrated over each control volume to obtain a set of discretized linear algebraic equations of the form:

$$a_p \varnothing_p = \sum a_{nb} \varnothing_{nb} + S_\varnothing \qquad (14)$$

The convective terms were approximated by the power scheme and the diffusive terms with the central differencing scheme. The SIMPLE algorithm of Patankar [**15**] was used to couple
continuity and momentum equations. The computational procedure is based on a collocated mesh, and the details can be found in the text by Ferziger and Peric [**16**]. The systems of algebraic equations are solved using the strongly implicit procedure (SIP) of Stone [**17**]. The computation is terminated when the residuals for the continuity and momentum equations get below 10^{-5} and the residual for the energy equation gets below 10^{-8}.

5. GRID SENSITIVITY TEST

The numerical scheme used to solve the governing equations for the present work is a finite volume approach. It provides a smooth solutions at the interior domain including the corners. The enclosure is meshed with a non- uniform rectangular grid with a very fine spacing near the walls. As shown in **Fig. 2**, the **2-D** computational grids are clustered towards the walls. The location of the nodes is calculated using a stretching function so that the node density is higher near the walls of the enclosure. Solutions are assumed to converge when the following convergence criteria is satisfied at every point in the solution domain :-

$$\left|\left(\phi_{new} - \phi_{nold}\right)/\phi_{old}\right| \leq 10^{-5} \qquad (15)$$

where ϕ represents a dependent variable **U, V, P,** and **θ**. In order to obtain grid independent solution, a grid refinement study is performed for ***Ra*** **= 10^4, Pr = 0.71,** and γ **= 0°.** In the present work, eight combinations (**80 x 80, 90 x 90, 95 x 95, 100 x 100, 150 x 150, 175 x 175**, **200 x 200** and **225 x 225**) of control volumes are used to test the effect of grid size on the accuracy of the predicted results. **Fig. 3** shows the convergence of the average Nusselt number, $\mathbf{Nu_{av}}$, at the heated surface with grid refinement. It is observed that grid independence is achieved with combination of **(100x100**) control volumes where there is insignificant change in $\mathbf{Nu_{av}}$. The agreement is found to be excellent which validates the present computations indirectly.

6. NUMERICAL RESULTS VERIFICATION

For the purpose of the present numerical algorithm verification, a laminar natural convection problem inside the same tested model as obtained by **Saha et al. [12]** considering a constant heat flux condition is performed. The comparison is made using the following parameters: **Pr = 0.71** , **Ra = 6 x 10^3** to **4 x10^4** , **E/L = 0.1, 0.3, 0.5** and **γ = 0°**. Comparisons of the average Nusselt numbers at a heated left side wall are shown in **Table 1**. A general agreement between the present computation values and the previous values by **Saha et al. [12]** is seen to be very well with a maximum deviation of about **4.42%.** Further validation is performed by using the present numerical algorithm to investigate the same problem considered by **Saha et al. [12]** using the same flow conditions, geometry, and the boundary conditions but the numerical scheme is different . The comparison is made using the following parameters: **Pr = 0.71**, **Ra = 10^3, E/L =0.1, 0.3, 0.5** and **γ = 0°**. Good agreement is achieved between **Saha et al.[12]** and the present numerical scheme for both the streamlines and temperature contours as shown in **Fig.4**. These validations make a good confidence in the present numerical model to deal with the same enclosure configuration problem but it is considered inclined to calculate the flow and thermal fields in the present work.

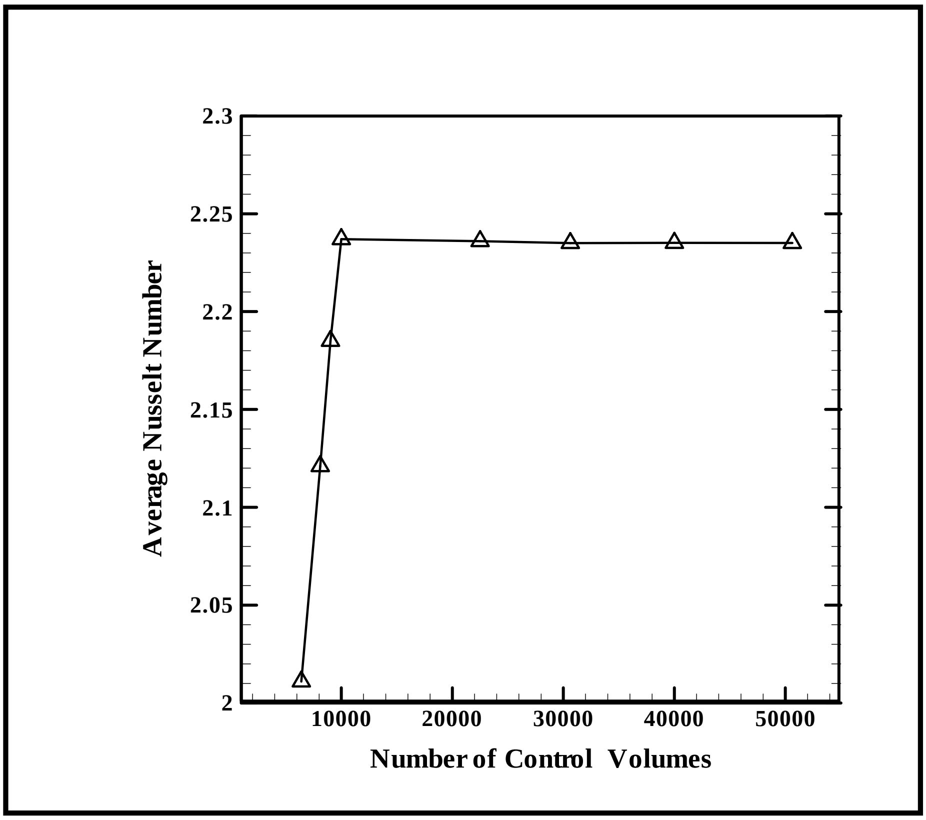

Fig. 3. Variation of average Nusselt number along the hot left side wall as a function of control volume for ***Ra* = 10^4, Pr= 0.71,** and **γ = 0°.**

Table 1

Comparison of the present average Nusselt number along the heated left side wall when enclosure inclination angle (γ) = 0° with those of previous studies at Pr = 0.71.

Ra	**E/L = 0.1**			**E/L = 0.3**			**E/L = 0.5**		
	Saha et al. [12]	**Present work**	**Error %**	**Saha et al. [12]**	**Present work**	**Error %**	**Saha et al. [12]**	**Present work**	**Error %**
6000	1.805	1.811	-2.16%	1.919	1.932	0.67%	1.975	1.968	-0.35%
8000	1.943	2.029	4.42%	2.061	2.027	-1.65%	2.119	2.122	0.14%
10000	2.056	2.041	-0.73%	2.176	2.168	-0.36%	2.235	2.237	0.08%
20000	2.436	2.448	0.49%	2.560	2.549	-0.43%	2.620	2.623	0.11%
40000	2.869	2.812	-1.98%	2.994	2.998	0.13%	3.053	3.044	-0.29%

7. RESULTS AND DISCUSSION

The characteristics of the flow and temperature fields in a square modified air-filled inclined enclosure are investigated in this section. In the present numerical investigation, the following ranges of the dimensionless groups are considered: The working fluid is air with Prandtl number(**Pr**) = **0.71,** the range of Rayleigh numbers **(** $\boldsymbol{Ra}$ **)** are $\mathbf{10^3}$, $\mathbf{10^4}$,$\mathbf{10^5}$ and $\mathbf{10^6}$ respectively while the enclosure inclination angle, γ, is varied as $\mathbf{0^o}$, $\mathbf{20^o}$**,** $\mathbf{40^o}$ and $\mathbf{60^o}$ respectively. **Figure 5** explains the variation of the streamlines and isotherms for inclination angle = **0°** when Rayleigh numbers $\boldsymbol{Ra}$ = $\mathbf{10^3}$, $\mathbf{10^4}$, $\mathbf{10^5}$ and $\mathbf{10^6}$ respectively and **E/L** ratio equals **0.1** ,**0.3** and **0.5** respectively. From this figure, the flow field is characterized by a primary recirculating air vortex near the left-hand wall where the temperature is high while its density is low due to the heat flux effect. This temperature and density differences between the left and right side walls causes this mentioned air vortex which filling most of the enclosure. When the range of Rayleigh numbers are low, the buoyancy force effect is small so for this case the convection heat transfer contribution is small. From the other hand when the Rayleigh number range increases**,** the buoyancy force effect becomes greater so the vortices shape becomes irregular due to the active fluid motion causing from the higher temperatures near the left-hand wall and as a result making a large convection heat transfer contribution. The figure also shows that the stream line contours are collect morly near the bottom wall than the top one due to the triangular shape of the top wall. In the same figure, the isotherm contours refer that the thermal field lines are almost linear and symmetrical at the upper part of the enclosure, so the diffusion heat transfer is dominated because the generated buoyancy force is not strong enough to initiate fluid convection. While the convection heat transfer is dominated at the lower part of the enclosure. When the Rayleigh number increases, the isotherms become non-symmetry ,uniform horizontally and linear vertically at the upper part of the enclosure. The results indicate also that the thermal boundary layers near the hot and cold side walls increases and concentrated as the effect of the Rayleigh number increases. **Figures (6**,**7** and **8)** explain the streamlines and isotherms contours in a modified square inclined enclosure which having a triangular top wall when the range of Rayleigh numbers **(** $\boldsymbol{Ra}$ **)** are $\mathbf{10^3}$, $\mathbf{10^4}$,$\mathbf{10^5}$ and $\mathbf{10^6}$ respectively, **E / L** ratio equals **0.1** ,**0.3** and **0.5** while the enclosure inclination angle, γ, is varied as **20^o** , **40^o** and **60^o** respectively. From these figures, the effect of inclination angle is small when the Rayleigh number is low. But when the Rayleigh number increases the fluid flow nature has a different behaviour where the fluid moving upwards in the interior of the enclosure and moving downwards in both the hot and cold side walls. The results indicate that the fluid internal motion near the left hot wall is more strong than that the opposite right cold wall. The reason of this behavior, is that the x-component of buoyancy effect due to external heating resulting from the temperature difference is small when the effect of inclination angle is small . From the other hand, the effect of x-component of buoyancy forces becomes more strong, as the inclination angle increases. The results show also that when the Rayleigh number is low, there is a primary recirculating vortex which covers most of the enclosure size. At ***Ra* = 10^6**, a two non-uniform recirculating vortices of different shape and opposite directions can be noticed. This irregularity in the vortices shape due to the flow confusion which causes a good convection heat transfer performance. Furthermore, the thermal field in the previous mentioned figures indicate that the isotherms lines are almost linear and symmetrical when the Rayleigh number is low, so the diffusion heat transfer is dominated. When the Rayleigh number increases, the isotherms become non-symmetry ,uniform horizontally and linear vertically at the upper part of the enclosure. Also, a thin thermal boundary layer is observed at the heated left side wall when the Rayleigh number and the inclination angle increases .Also, these figures indicate that when **E / L** ratio increases together with the increase in the Rayleigh number and the inclination angle, the spacing near the triangular inclined top walls decreases and the flow field enlarge to cover all the enclosure zone. The reason of this behaviour is that due to the increase in the flow velocity and a large surface area due to the increase of **E/L** ratio. The variation of the average Nusselt number along the hot left side wall is explained in **Figure 9** when the range of Rayleigh numbers **(*Ra*)** are **10^3**, **10^4** ,**10^5** and **10^6** respectively, **E / L** ratio equals **0.1** ,**0.3** and **0.5** while the enclosure inclination angle, γ, is varied as **0^o**, **20^o**, **40^o** and **60^o** respectively. The figure explains that when the **E/L** ratio is high, the average Nusselt number increases together with the increase in the Rayleigh number and the inclination angle. This is due to the increase in the intensity of convection currents which causes a clear change in the heat transfer rate.

8. CONCLUSIONS

The following conclusions can be drawn from the results of the present work:

1-When the inclination angle is $\mathbf{0^o}$ and the Rayleigh numbers are low, the buoyancy force effect is small and the convection heat transfer contribution is small.

2-When the Rayleigh number increases**,** the vortices shape becomes irregular and making a large convection heat transfer contribution.

3- When the inclination angle is $\mathbf{0^o}$ the isotherm contours refer that the thermal field lines are almost linear and symmetrical at the upper part of the enclosure, so the diffusion heat transfer is dominated .While the convection heat transfer is dominated at the lower part of the enclosure.

4-When the Rayleigh number increases, the isotherms become non-symmetry ,uniform horizontally and linear vertically at the upper part of the enclosure.

5- When the inclination angle is increased, the effect of inclination angle is small when the Rayleigh number is low. But when the Rayleigh number increases the fluid flow nature has a clear different behaviour.

6- When the Rayleigh number is low, there is a primary recirculating vortex which covers most of the enclosure size. At $\boldsymbol{Ra} = \mathbf{10^6}$, a two non-uniform recirculating vortices of different shape and opposite directions can be noticed.

7- When **E/ L** ratio increases with the increase in the Rayleigh number and the inclination angle,the spacing near the triangular inclined top walls decreases and the flow field enlarge to cover all the enclosure zone.

8- When the **E/L** ratio is high, the average Nusselt number increases with the increase in the Rayleigh number and the inclination angle.

9. REFERENCES

[1]- Saha , G. ,Saha ,S.and Mamun , M. ,2007. “A Finite Element Method for Steady State Natural Convection In a Square Tilt Open Cavity ”, ARPN Journal of Engineering and Applied Sciences, Vol. 2, No. 2, pp: 41–49.

[2]- Ali, M. and Husain, S. R., 1993. “Effect of Corrugation Frequencies on Natural Convective Heat Transfer and Flow Characteristics in a Square Enclosure of Vee-Corrugated Vertical Walls”, International Journal of Energy Research ,Vol.17, pp: 697-708.

[3]- Ganzarolli, M. and Milanez, L., 1995. “Natural Convection in Rectangular Enclosures Heated from Below and Symmetrically Cooled from the Sides”, International Journal of Heat and Mass Transfer, Vol. 38, pp: 1063–1073.

[4]- Aydin, O. and Yang, J., 2000. “Natural Convection in Enclosures with Localized Heating from Below and Symmetrical Cooling from Sides”, International Journal of Numerical Methods in Heat and Fluid Flow, Vol.10, pp: 518–529.

[5]- Sharif, M. and Mohammad, T., 2005. “Natural Convection in Cavities with Constant Flux Heating at the Bottom Wall and Isothermal Cooling from the SideWalls”, International Journal of Thermal Sciences,Vol.44, pp: 865-878.

[6]- Sivasankaran, I., 2006. “Buoyant Convection in a Cavity with Discreate Heat Sources and Internal Heat Generation”, International Journal of Applied Mathematics and Mechanics,Vol.2, No.2, pp:63-74.

[7]- Kandaswamy, P. and Sivasankaran, S. ,2006.“Natural Convection in an Inclined Enclosure with Internal Heat Generation”, Proceedings of the National Academy of Sciences, India,Vol.76(A) , pp: 145–150.

[8]- Sathiyamoorthy, M. ,Tanmay Basak, B., Roy, S. and Pop, I., 2007. “Steady Natural Convection Flows in a Square Cavity with Linearly Heated Side Wall(s)”, International Journal of Heat and Mass Transfer, Vol.50, pp:766-775.

9]- Kandaswamy, P., Lee, J. and Abdul Hakeem, A., 2007."Natural Convection in a Square Cavity in the Presence of Heated Plate", Nonlinear Analysis: Modelling and Control , Vol. 12, No. 2, pp:203–212.

[10]- Natarajan, E., Tanmay Basak, B. and Roy, S. , 2008. "Natural Convection Flows in a Trapezoidal Enclosure with Uniform and Non-Uniform Heating of Bottom Wall ", International Journal of Heat and Mass Transfer, Vol.51, pp:747-756.

[11]- Sultana, T., Saha, S., Saha, G. and Quamrul Islam, M., 2008. "Natural Convection in Tilted Square Cavities with Triangular Shaped Top Cold Wall ", Journal of Mechanical Engineering ,Vol. ME 39,No.1, pp: 33–42.

[12]-Saha, S., Hasan, N. and Feroz, C., 2008. "Natural Convection in a Differentially Heated Enclosure with Triangular Roof ", Journal of Mechanical Engineering ,Vol. ME 39,No.1, pp: 1–7.

[13]- Thompson, P., Thamas, F. and Mastin, F., 1974. "Automatic Numerical Generation of Body- Fitted Curvilinear Coordinate System" Journal of computational physics, Vol. 15, pp: 299-319.

[**14**]- Thomas, P. D. and Middlecoff, J. F., 1980." Direct Control of The Grid Point Distribution In Meshes Generated by Elliptic Equations" , AIAA Journal , Vol. 18, No. 6, pp: 652-656.

[15]- Patankar, S.V., 1980. "Numerical Heat Transfer and Fluid Flow" , Hemisphere Publishing Corporation, New York.

[16]-Ferzinger, J. and Peric, M., 1999. "Computational Methods for Fluid Dynamics", 2nd edition Springer Verlag, Berlin Hedelberg.

[17] Stone, H. L., 1968. "Iterative Solution of Implicit Approximations of Multidimensional Partial Differential Equations", SIAM J. Numer. Anal., vol. 5, pp. 530–558,

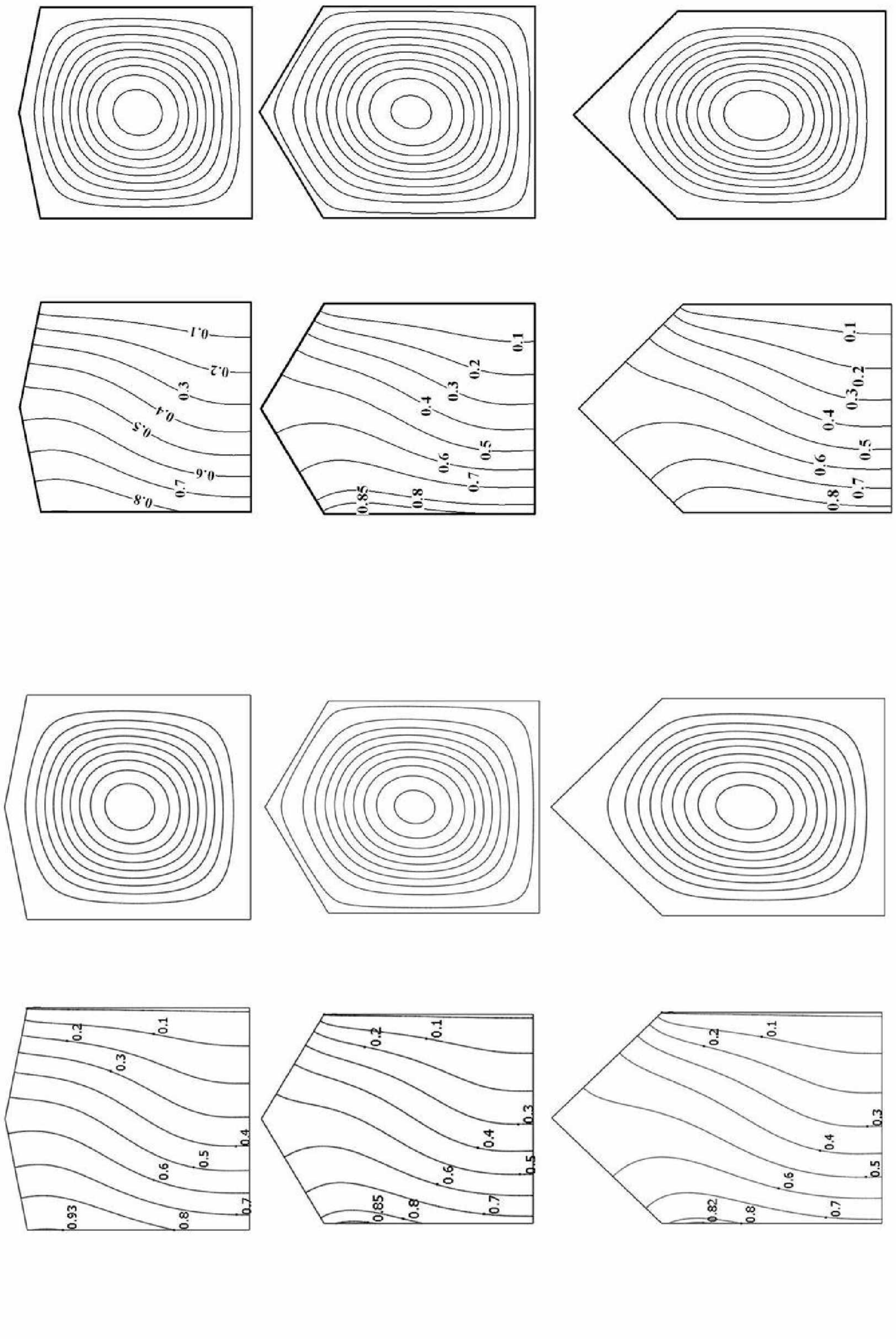

Fig. 4. Comparison of the isotherms and streamlines between the present work (right) and that of Saha et al. [12] (left) in the modified square enclosure air -filled using the flow conditions (Pr = 0.71, $Ra = 10^3$, $\gamma = 0°$)

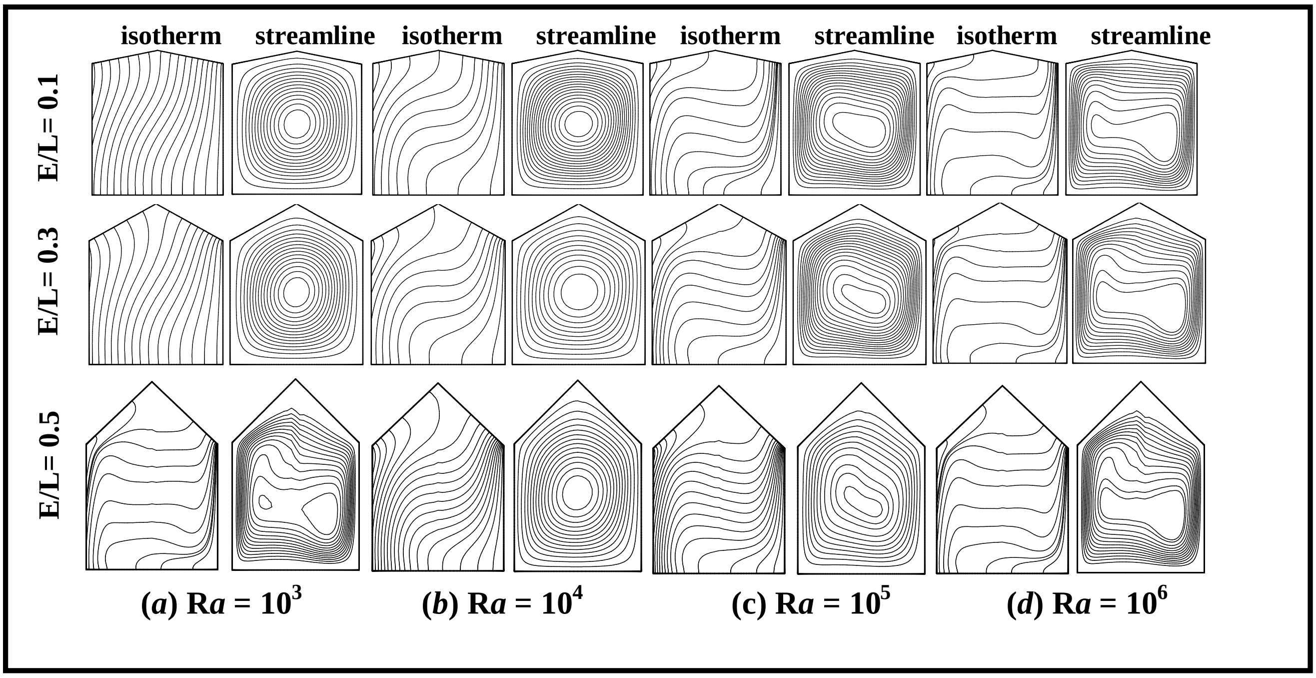

Figure 5: Isotherm and Streamline Patterns for Rayleigh Numbers, (*a*) R*a* = 10^3, (b) R*a* = 10^4, (c) R*a* = 10^5, (d) R*a* = 10^6 at inclination angle = 0°.

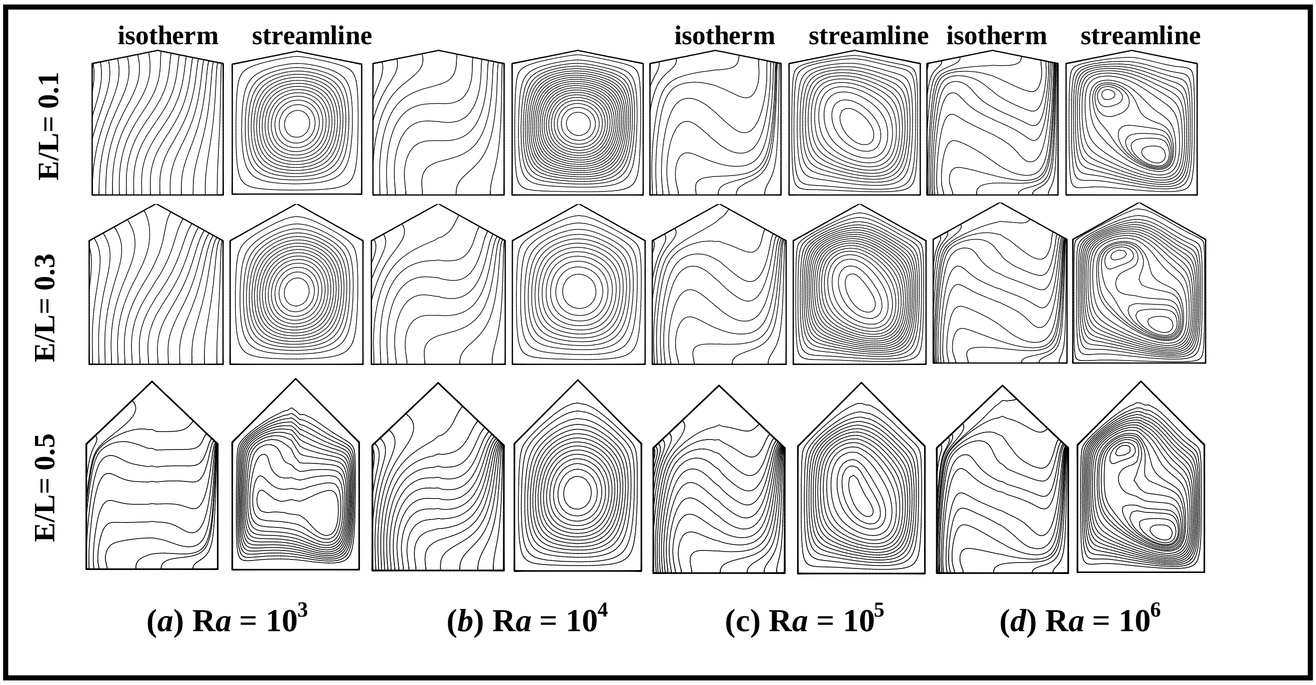

Figure 6: Isotherm and Streamline Patterns for Rayleigh Numbers, (*a*) R*a* = 10^3, (b) R*a* = 10^4, (c) R*a* = 10^5, (d) R*a* = 10^6 at inclination angle = 20°.

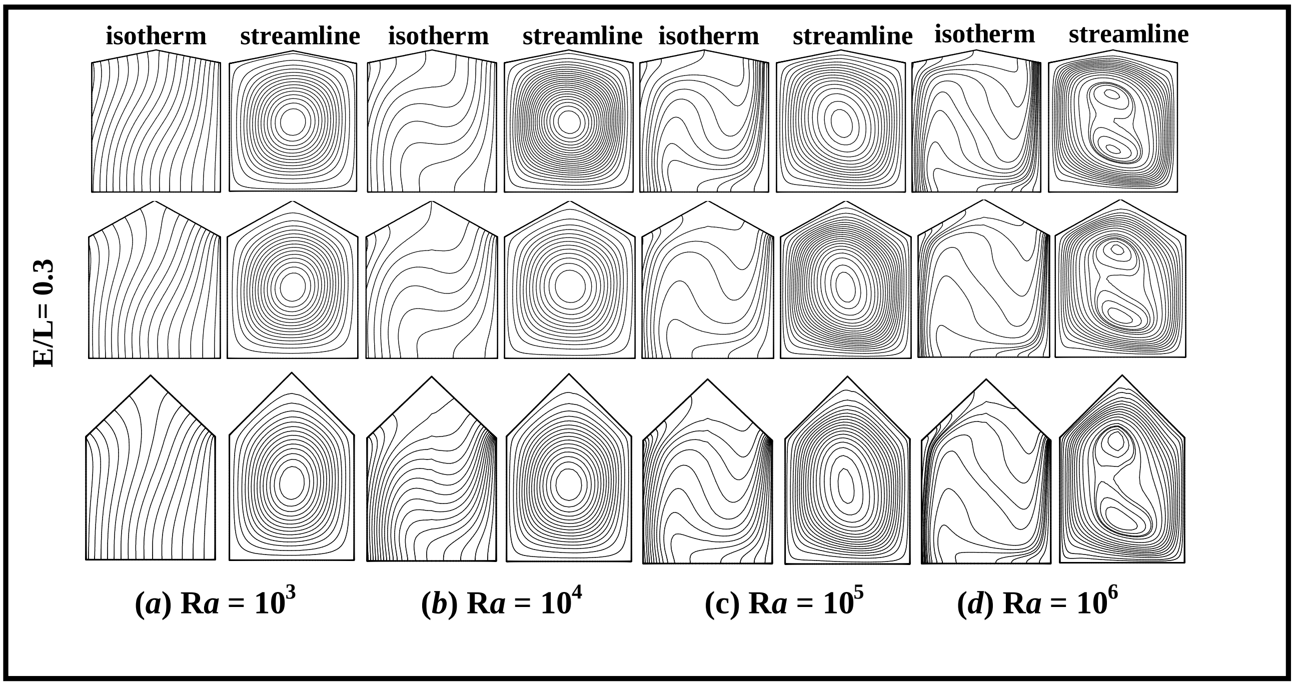

Figure 7: Isotherm and Streamline Patterns for Rayleigh Numbers, (*a*) R*a* = 10^3, (b) R*a* = 10^4, (c) R*a* = 10^5, (d) R*a* = 10^6 at inclination angle = 40°.

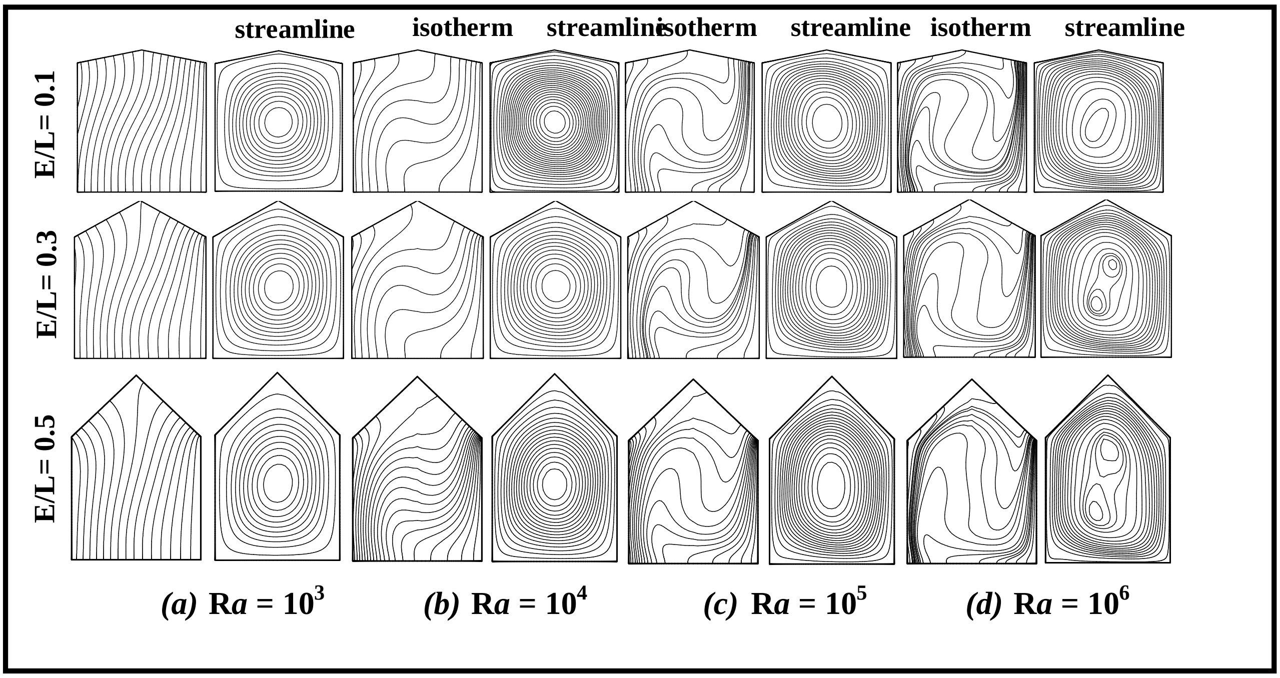

Figure 8: Isotherm and Streamline Patterns for Rayleigh Numbers, (*a*) R*a* = 10^3, (b) R*a* = 10^4, (c) R*a* = 10^5, (d) R*a* = 10^6 at inclination angle = 60°.

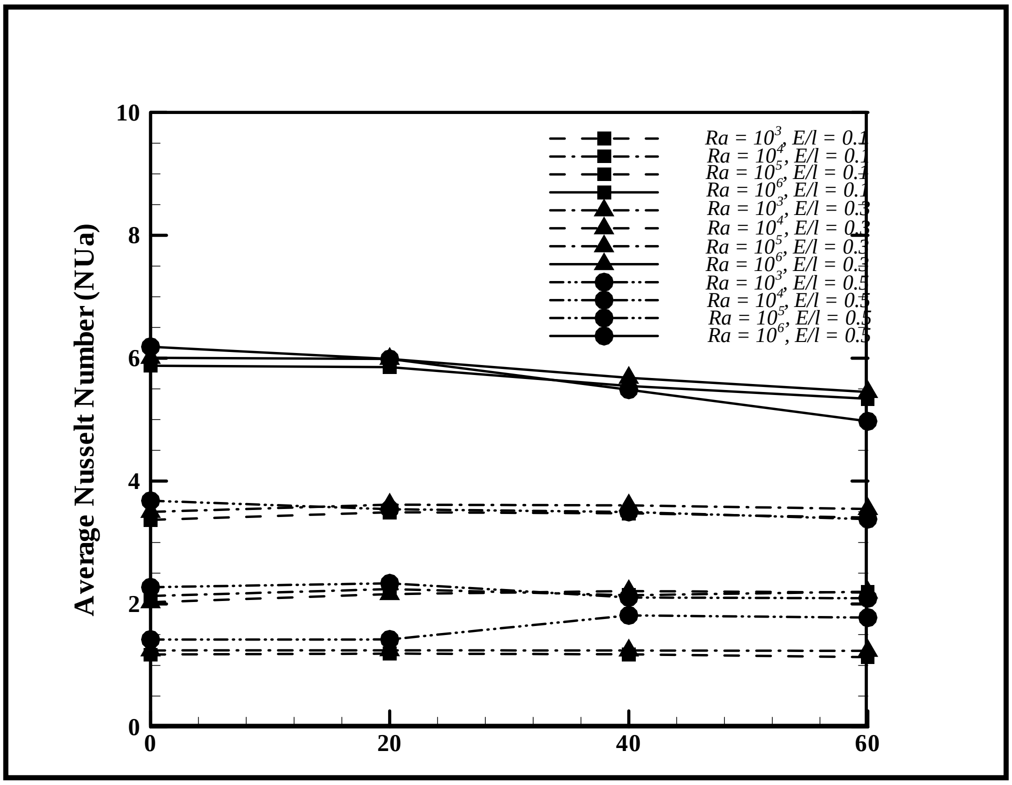

Fig. 9. Variation of The Average Nusselt Number along The Heated Left Side Wall With Inclination Angles of The Modified Square Enclosure For Different Inclined Roof Heights and Rayleigh Numbers